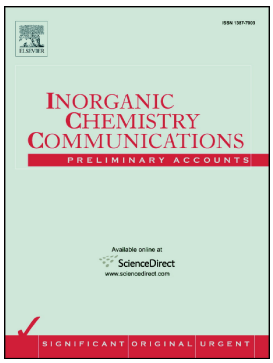

Design, synthesis, crystal structure and cytotoxicity studies of colorimetric fluorescent "OFF-ON" probes for rapid detection of hydrogen sulfide based on Cu(II) complex

Xuefang Shang, Xuejing Yue, Yanmei Chen, Congshu Li, Hongli Chen, Tianyun Wang

PII: S1387-7003(18)30876-1
DOI: https://doi.org/10.1016/j.inoche.2018.10.030
Reference: INOCHE 7164

To appear in: *Inorganic Chemistry Communications*

Received date: 21 September 2018
Revised date: 31 October 2018
Accepted date: 31 October 2018

Please cite this article as: Xuefang Shang, Xuejing Yue, Yanmei Chen, Congshu Li, Hongli Chen, Tianyun Wang , Design, synthesis, crystal structure and cytotoxicity studies of colorimetric fluorescent "OFF-ON" probes for rapid detection of hydrogen sulfide based on Cu(II) complex. Inoche (2018), https://doi.org/10.1016/j.inoche.2018.10.030

Design, synthesis, crystal structure and cytotoxicity studies of colorimetric fluorescent "OFF-ON" probes for rapid detection of hydrogen sulfide based on Cu(Ⅱ) complex

Xuefang Shang[a]*, Xuejing Yue[b], Yanmei Chen[a], Congshu Li[a], Hongli Chen[c], Tianyun Wang[d]

[a]Key Laboratory of Medical Molecular Probes, Department of Chemistry, School of Basic Medical Sciences, Xinxiang Medical University, Xinxiang, Henan 453003, China

[b]Clinical skills training center，Xinxiang Medical University，Xinxiang，China，453003, China

[c]School of Life Science and Technology, Xinxiang Medical University, Xinxiang, Henan 453003, China

[d]Department of Biochemistry and Molecular Biology, Xinxiang Medical University, Xinxiang, Henan 453003, China

*Corresponding author: Tel +86-373-3029128, Fax +86-373-3029959

E-mail: xuefangshang@126.com

Abstract: Four colorimetric fluorescent probes based on copper(II) complexes were synthesized and the molecular structures were characterized by X-ray diffraction, ESI-HRMS and elemental analysis. When exposed to HS^-, the synthesized probes showed significant color changes from yellow to red and remarkable increase of fluorescence intensity (over 80-fold). What's more, the interaction of host-guest could be completed in 2 minutes. However, no clear color and fluorescence intensity changes were observed in the presence of other anions (AcO^-, $H_2PO_4^-$, F^-, Cl^-, Br^-, I^-, SO_4^{2-}, SO_3^{2-}, CO_3^{2-}, Cys and GSH). The synthesized colorimetric fluorescent probes could detect HS^- rapidly and conveniently. Cytotoxicity studies indicated that the synthesized fluorescent probes were low cytotoxicity in Hela cells and may be used to detect H_2S level in *vivo*.

Key words: hydrogen sulfide; fluorescent probe; colorimetric detection; cytotoxicity; copper complex crystal

1. Introduction

It is well known that hydrogen sulfide (H_2S) is the rotten egg smell and considered merely as a toxin with no beneficial physiological significance in the past years. With the initial observation by Kimura's group, H_2S is an important signaling molecule as the biological relevance [1]. Followed by carbon monoxide(CO) and nitric oxide(NO), H_2S is identified as the third member of the gasotransmitter family [2-6]. Some literatures reported that H_2S usually appeared in various physiological processes, including relaxation of vascular smooth muscles, mediation of neurotransmission, regulation of inflammation and O_2 sensing, and also could protect against ischemia/reperfusion injury [7-10]. Besides, the abnormal level of H_2S was linked to some diseases such as Huntington's disease (HD), Down's syndrome, diabetes and liver cirrhosis [11-15]. Therefore, the detection research on H_2S, intriguing gas, showed the potential therapeutic implication in the biological and pathological process [16]. However, the above aspect is still in its infancy. The quantified detection of H_2S in living cells is crucial in order to understand its biological and pathological roles.

So far, many traditional methods have been reported for the detection of H_2S including electrochemistry, chemiluminescence, chromatography, and methylene blue assay [17-19]. The above methods are generally limited because of their invasive and destructive nature to the living organisms. On the other hand, small fluorescent probes have attracted the most attention for sensing and visualizing analytes in living cells because fluorescent probes exhibited many advantages such as high sensitivity and

good cell permeability [20-36]. A few small molecular fluorescent turn-on probes [37-41] and ratiometric probes [42, 43] have been successfully developed based on the H_2S-induced specific reactions, such as displacement method [44-46], reduction of azide [47], nucleophilic reaction [48]. And some of the above methods have been used for intracellular H_2S imaging [49] which can provide real-time, easy-to-use, nondestructive detection in live cells or tissues.

Based on the above considerations, we designed and synthesized a series of copper(Ⅱ) complex (Scheme 1) to study the anion binding ability, especially for HS^- detection. In addition, bromine group and naphthylamine acted as colorimetric group and fluorometric group respectively. Fortunately, the crystals of the copper complexes were also obtained. As expected, the synthesized complexes showed the strong binding ability for HS^- (a commonly employed H_2S donor) among the tested anions (HS^-, AcO^-, $H_2PO_4^-$, F^-, Cl^-, Br^-, I^-, SO_4^{2-}, SO_3^{2-}, CO_3^{2-}, Cys and GSH).

2. Material and methods

2.1 Experiment

Unless otherwise specified, all materials and solvents were of analytical grade. Sodium hydrosulfide hydrate, all anions in the form of tetrabutylammonium salts (such as $(n\text{-}C_4H_9)_4NCl$, $(n\text{-}C_4H_9)_4NBr$, $(n\text{-}C_4H_9)_4NI$, $(n\text{-}C_4H_9)_4NAcO$, $(n\text{-}C_4H_9)_4NH_2PO_4$, NaHS, Na_2SO_4, Na_2SO_3, Na_2CO_3, Cys and GSH) were purchased from Aladdin Chemistry Co. Ltd (Shanghai, China). All anions were stored in a desiccator under vacuum. Dimethyl sulfoxide (DMSO) was distilled in vacuum after being dried with CaH_2. ^1H NMR spectra were recorded using a Bruker Ascend^{TM} 400 spectrometer with chemical shifts reported as ppm with TMS as internal standard. ESI-HRMS was performed using a Bruker Microtof-QIII spectrophotometer. UV-vis titration experiments were carried using a Shimadzu UV2600 Spectrophotometer at

298 K. Fluorescence spectra were measured using an Eclipse fluorescence spectrophotometer (Agilent, USA). The binding constant, K_s, was obtained by non-linear least squares calculation method for data fitting.

For cytotoxicity test, the living Hela cells were seeded into a 96-well plate at a density of 5×10^4 cells/well. After the cells form monolayer, the culture media was replaced by the complex solution (2.5-80 μg·mL^{-1}). After incubated for 24 h, complex solution was then replaced with fresh media after several washing steps, and 20 μL MTT (5 mg·mL^{-1}) was added to each well and incubated for a further 4 h in humidified atmosphere. After that, the culture media was removed and the solvent (DMSO, 150 μL) was then added. Finally, the absorbance of cells was detected at 490 nm using the microplate reader (Thermo Multiscan MK3, Thermo Fisher Scientific, MA, USA) with the plain cell culture media as the control. Cell viability was expressed by the ratio between the absorbance of the cells incubated with complex and that of blank culture media.

2.2 Synthesis

*2.2.1 Bis(3,5-dibromosalicylidene-aniline) copper(II) (compound **1**)*

3, 5-dibromosalicylidene-aniline was synthesized according to the literature [50]. It was obtained by refluxing the ethanol solution (40 mL) of 3, 5-dibromosalicyl-aldehyde (10 mmol, 2.8 g) and phenylamine (10 mmol, 930 mg) for 4 h and the yellow precipitate was recrystalled by ethanol, washed with water, and dried under vacuum. Yield: 85%. m.p. 102.5-104.0 ℃. ^{1}H NMR (400 MHz, $CDCl_3$) δ 14.53 (s, 1H, -OH), 8.57 (s, 1H, -CH=N-), 7.78 (d, J = 2.3 Hz, 1H, ph-H), 7.52 (d, J = 2.3 Hz, 1H, ph-H), 7.48 (dd, J = 10.6, 4.9 Hz, 2H, ph-H), 7.40 – 7.30 (m, 3H, ph-H) (**S1)**. ESI-MS (m/z): 354.0 (*M*-H)$^-$.

Bis(3,5-dibromosalicylidene-aniline*)* copper*(II)* (compound **1**) was synthesized according to the following procedure. Copper acetate hydrate (99 mg, 0.5 mmol) was added to a stirred solution of 3, 5-dibromosalicylideneaniline (355 mg, 1 mmol) in ethanol (15 mL). The mixture was stirred for 1 h at 55 ℃, and then stood overnight at room temperature. Suitable brown single crystal for X-ray crystal structural analysis was obtained, separated by filtration, washed with cyclohexane. Yield: 82%. m.p. 251.8 – 254.2 ℃. ESI-HRMS (m/z): 789.7123 $(M+Na)^+$ (**S5)**.

*2.2.2 Bis(5-bromosalicylidene-aniline) copper(II) (compound **2**)*

The synthesis method was similar to the above procedure. 5-bromosalicylideneaniline Yield: 75%. m.p. 121.3 - 123.1 ℃. ^{1}H NMR (400 MHz, $CDCl_3$) δ 13.31 (s, 1H, -OH), 8.58 (s, 1H, -CH=N-), 7.54 (d, J = 1.5 Hz, 1H, ph-H), 7.47 (t, J = 7.6 Hz, 3H, ph-H), 7.35 (d, J = 6.9 Hz, 1H, ph-H), 7.31 (s, 1H, ph-H), 7.29 (s, 1H, ph-H), 6.96 (d, J = 8.8 Hz, 1H, ph-H) (**S2**). ESI-MS (*m/z*): 274.0 $(M-H)^-$.

Bis(5-bromosalicylideneaniline) copper(II) (compound **2**). Yield: 82%. m.p. 282-284℃. ESI-HRMS (m/z): 633.9071 $(M+Na)^+$ (**S6**).

*2.2.3 Bis(3,5-dibromosalicylidene-α-Naphthylamine) copper(II) (compound **3**)*

The synthesis method was similar to the above procedure. 3, 5-dibromosalicylid-ene-*α*-Naphthylamine Yield: 75%. mp. 151. 4 -153.2 ℃. ^{1}H NMR (400 MHz, $CDCl_3$) δ 14.75 – 14.19 (m, 1H, -OH), 8.66 (s, 1H, -CH=N-), 8.28 – 8.23 (m, 1H, ph-H), 7.92 (dt, J = 5.2, 3.0 Hz, 1H, ph-H), 7.87 (d, J = 8.3 Hz, 1H, naphthyl-H), 7.83 (d, J = 2.3 Hz, 1H, ph-H), 7.62 – 7.57 (m, 3H, naphthyl-H), 7.57 – 7.50 (m, 1H, naphthyl-H), 7.24 (dd, J = 7.3, 0.9 Hz, 1H, naphthyl-H) (**S3**). ESI-MS (*m/z*): 404.0 $(M-H)^-$.

*2.2.4 Bis(5-bromosalicylidene-α-Naphthylamine) copper(II) (compound **4**)*

The synthesis method was similar to the above procedure. 5-bromosalicylidene-α-Naphthylamine Yield: 75%. m.p. 108 - 110 ℃. ^{1}H NMR (400

MHz, $CDCl_3$) δ 13.44 (s, 1H, -OH), 8.66 (s, 1H, -CH=N-), 8.24 (dt, J = 6.8, 3.4 Hz, 1H, ph-H), 7.95 – 7.87 (m, 1H, ph-H), 7.84 (d, J = 8.3 Hz, 1H), 7.60 (s, 1H, naphthyl-H), 7.58 (t, J = 2.9 Hz, 1H, naphthyl-H), 7.56 – 7.48 (m, 2H, naphthyl-H), 7.28 (s, 1H, ph-H), 7.20 (dd, J = 7.3, 0.7 Hz, 1H, naphthyl-H), 7.03 (d, J = 8.8 Hz, 1H, naphthyl-H) (**S4**). ESI-MS (*m/z*): 324.0 $(M\text{-H})^-$.

Bis(5-bromosalicylidene-α-Naphthylamine) copper(II) (compound **4**). Yield: 75%. ESI-HRMS (m/z): 733.9186 $(M\text{+Na})^+$ (**S7**).

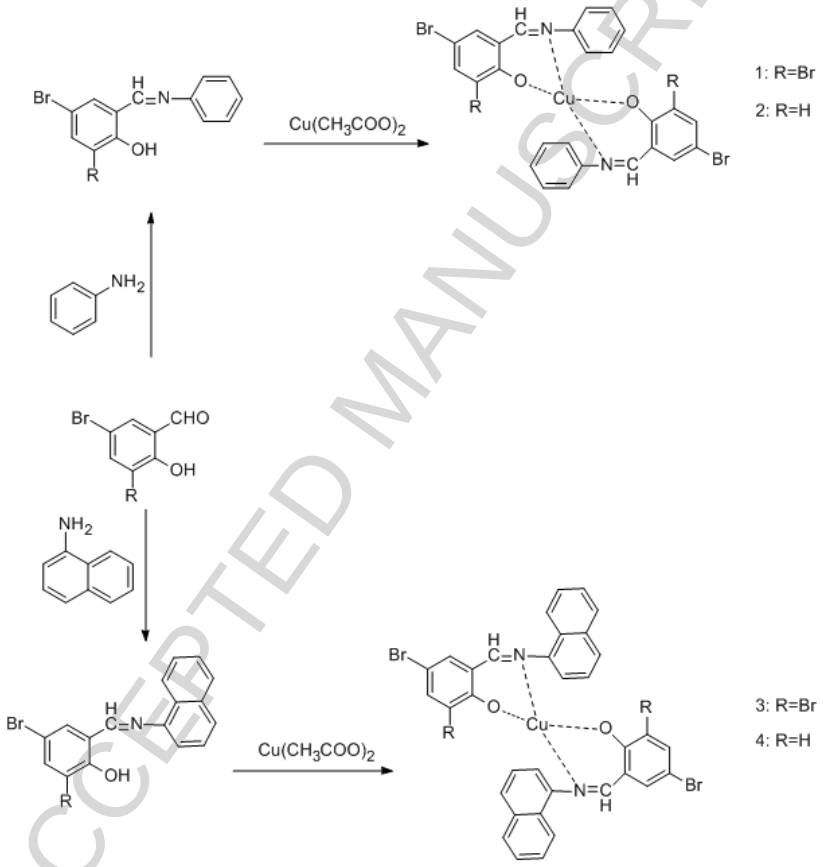

Scheme 1 Synthesis route for Copper(Ⅱ) Complexes

3. Results and discussion

3.1 X-ray crystal structure

Single crystals of synthesized complexes (**1**-**4**) were all obtained at room temperature from the ethanol solvent by slow evaporation. In order to confirm the chemical structure of the complex, single crystal X-ray analysis was used to

determine the structure of the copper complex. Parameters in CIF format are available from Cambridge Crystallographic Date Center (CCDC 1432286 1432284 1448106 and1432281). The molecular structures of the copper complexes with the atoms numbering scheme were given in Fig. 1. The detailed summary of the crystal data was given in Table 1. Selected bond lengths and bond angles were listed in Table 2.

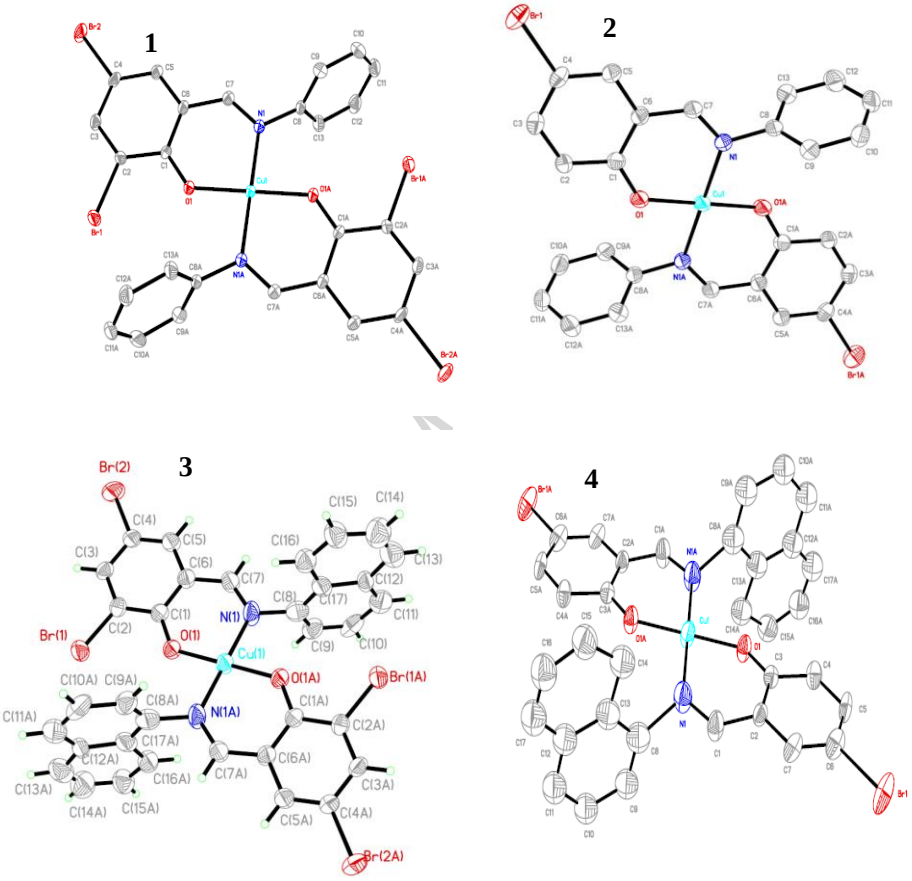

Fig.1 The ORTEP view of copper complexes (**1**-**4**)

The bond angles were all fit with the ideal value (180°). The crystallographic data revealed that the metal center was four-coordinated system by two oxygen and nitrogen atoms in two Schiff base ligands. The bond (Cu–O) was in trans- configuration and the distance (Cu–O) was shorter than the distance (Cu–N). The Schiff base lost a proton from the hydroxyl group and acted as a single charged bidentate ligand coordinating to copper(II). The ligands coordinated to the Cu(II)

center in trans- orientation with respect to each other. The geometry around the metal center was a distorted square-planar, with P21/c space group. All these parameters were in close agreement with those reported for square planar copper(II) compounds [51-53].

Table 1. Crystal data and structure refinement for complexes

Compound	**1**	**2**	**3**	**4**
Empirical formula	C26H16Br4 CuN2O2	C26H18Br2 CuN2O2	C34H20Br4 CuN2O2	C34H22Br2 CuN2O2
Formula weight	771.59	613.78	871.70	713.9
T (K)	296(2)	296(2)	153(2)	296(2)
λ (Å)	0.71073 Å	0.71073	0.71073	0.71073
Crystal system	monoclinic	monoclinic	tetragonal	monoclinic
Space group	P21/c	P21/n	P21c	P21/c
Crystal color	Brown	Brown	Brown	Brown
Crystal size mm × mm × mm	0.370 x 0.251 x 0.202	0.261 x 0.219 x 0.086	0.21 x 0.10 x 0.10	0.20 x 0.16 x 0.06
a (Å)	10.3880(11)	9.7702(5)	11.1806(12)	11.628(2)
b (Å)	9.5412(9)	9.8852(5)	10.8307(11)	9.7474(19)
c (Å)	13.0905(12)	13.2482(6)	13.2203(13)	13.809(3)
α (°)	90	90	90	90
β (°)	103.789(3)	110.7396(16)	112.718(3)	114.33(3)
γ (°)	90	90	90	90
V (Å3)	1260.1(2)	1196.60(10)	1476.7(3)	1426.1(5)
μ (mm−1)	7.237	4.278	6.188	3.603
Dcalc (g/mL)	2.034	1.704	1.960(1)	1.662
Z	2	2	2	2
F(0 0 0)	742	606	846	710
θ range for data collection (°)	3.108 to 27.53	3.036 to 27.54	3.16 to 25.00	3.24 to 24.50
Index ranges	$-13 \leqslant h \leqslant 13$	$-12 \leqslant h \leqslant 12$	$-13 \leqslant h \leqslant 13$	$-13 \leqslant h \leqslant 13$
	$-12 \leqslant k \leqslant 12$	$-11 \leqslant k \leqslant 12$	$-12 \leqslant k \leqslant 12$	$-11 \leqslant k \leqslant 11$
	$-17 \leqslant l \leqslant 16$	$-17 \leqslant l \leqslant 17$	$-15 \leqslant l \leqslant 15$	$-16 \leqslant l \leqslant 16$
Maximum and minimum transmission	0.053 and 0.018	0.692 and 0.341	0.5823 and 0.3593	0.8183 and 0.5313
Refinement method	Full-matrix least-squares on F^2	Full-matrix least-squares on F^2	Full-matrix least-squares on F^2	Full-matrix least-squares on F^2
Goodness-of-fit on F2	1.010	1.076	1.029	1.293
R1 and wR2 indices [I > 2σ(I)]	R1 = 0.0456, wR2 = 0.1260	R1 = 0.0504, wR2 = 0.1369	R1 = 0.0617, wR2=0.1431	R1 = 0.0966, wR2 =0.2163
R1 and wR2 indices (all data)	R1 = 0.0523, wR2 = 0.1351	R1 = 0.0782, wR2 = 0.1607	R1 = 0.1128, wR2=0.1680	R1 = 0.2123, wR2 =0.2583
Largest difference in peak and hole (e Å−3)	1.579 and -1.004	0.935 and -0.723	0.972 and -0.393	0.917 and -0.432

Table 2. Selected bond lengths (Å) and angles (°) for the complexes (**1**-**4**)

Bond length(Å)	Angles (°)			
	1	**2**	**3**	**4**
Cu(1)-O(1)	1.896(2)	1.882(2)	1.891(4)	1.861(7)
Cu(1)-O(1)#1	1.896(2)	1.882(2)	1.891(4)	1.861(7)
Cu(1)-N(1)	2.014(3)	1.992(3)	2.001(7)	1.996(9)
Cu(1)-N(1)#1	2.014(3)	1.992(3)	2.001(7)	1.996(9)
O(1)#1-Cu(1)-O(1)	180.00(15)	180.0	180.0(1)	180.0(1)
N(1)-Cu(1)-N(1)#1	180.00(15)	180.0	180.0(1)	180.0(1)
O(1)-Cu(1)-N(1)	91.83(11)	91.63(11)	91.3(2)	90.4(3)
O(1)#1-Cu(1)-N(1)#1	91.83(11)	91.63(11)	91.3(2)	90.4(3)
O(1)#1-Cu(1)-N(1)	88.17(11)	88.37(11)	88.7(2)	89.6(3)
O(1)-Cu(1)-N(1)#1	88.17(11)	88.37(11)	88.7(2)	89.6(3)

Symmetry transformations used to generate equivalent atoms: #1 -x+2,-y,-z+2

3.2 UV-vis titration

The binding abilities of copper complexes with anions were investigated using UV-vis absorption spectra in DMSO and DMSO-H_2O (9:1, v/v) at 298 K. The UV-vis spectral changes of copper complex **1** (8.0×10^{-5} mol·L^{-1} in DMSO) were shown in Fig. 2. It was clear that the maximal absorption band of complex **1** at 390 nm was shifted to the long wavelength gradually with the increasing amount of HS^-. The wavelength shifted to 430 nm when 1.0 equiv. of HS^- was added. Three clear isosbestic points at 312, 374 and 420 nm suggested that complex **1** interacted with HS^- which host-guest complex informed each other. When 8 equiv. of HS^- was added, the maximal absorption band shifted to the long wave direction at 530 nm. At the same time, one isosbestic point at 476 nm appeared and the intensity of new absorbance peak enhanced by 46 times. The reason for red-shift phenomenon ($\Delta\lambda$=140 nm) may be link with the introduction of bromine, acting as colorimetric group. In addition, the color change of complex **1** solution could be observed from yellow to red (Fig. 4)

upon the addition of HS^- anion. The above results indicated that the synthesized com-

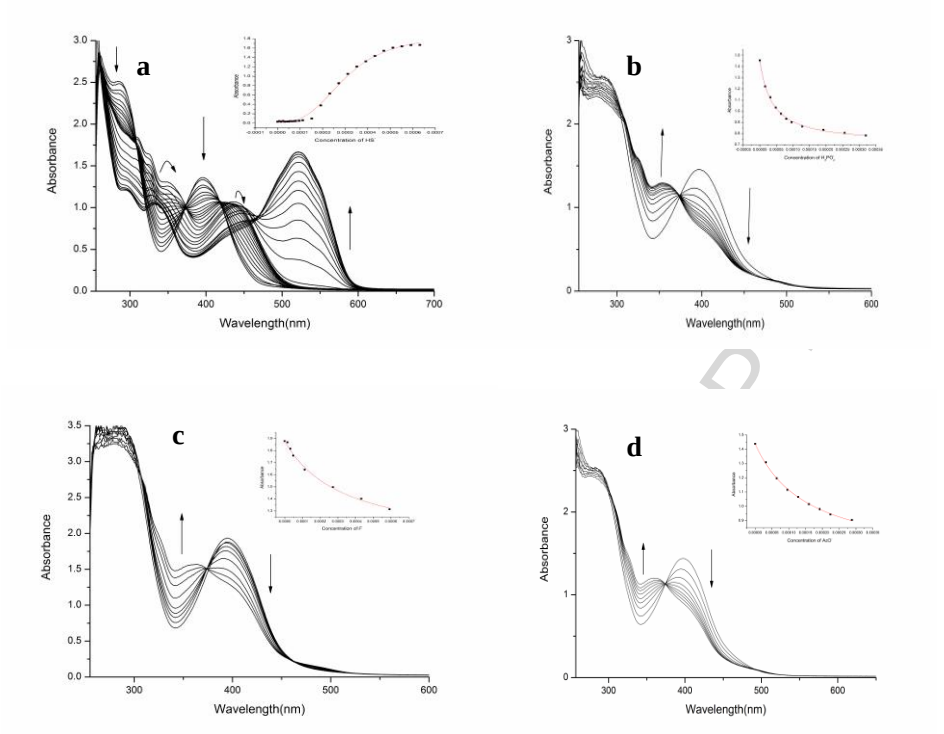

Fig. 2 UV-vis spectral changes of complex **1** upon the addition of various anions. [complex] = 8.0×10^{-5} mol·L^{-1} in DMSO: (a)HS^-, (b)$H_2PO_4^-$, (c)F^-, (d)AcO^-. Arrows indicate the direction of increasing anions concentration.

plex **1** may be used as colorimetric probe for the HS^- detection. For an excellent fluorescent probe, high selectivity is very important. Analogous investigations were carried out on other normal anions. The additions of $H_2PO_4^-$, AcO^- and F^- to complex **1** induced a blue-shift from 400 nm to 360 nm which indicated complex **1** also interacted with the above anions. While, the interacted mechanism of complex **1** with $H_2PO_4^-$, AcO^- and F^- was different from HS^- due to the different wave-shift phenomenon. The additions of Cys and induced the weak similar spectral changes. However, the additions of Cl^-, Br^-, I^-, SO_4^{2-}, SO_3^{2-}, CO_3^{2-} and GSH did not induce any spectral responses which indicated that complex **1** showed almost no binding abilities toward these anions or the binding abilities were very weak and could be

ignored. UV-vis absorption spectra changes of complex **3** were similar to that of **1** which the intensity of absorption peak at 400 nm decreased gradually and a new absorption peak at 520 nm increased upon the additions of HS^-, $H_2PO_4^-$, AcO^- and F^- anions (**S8**). In addition, the interaction process accompanied with color changes. The addition of Cys also induced similar spectral changes which the responses were weaker than HS^-. The above results indicated that complex **3** also interacted with HS^-, $H_2PO_4^-$, AcO^-, F^-, Cys and GSH as different binding ability and also no binding ability for Cl^-, Br^-, I^-, SO_4^{2-}, SO_3^{2-} and CO_3^{2-}.

Similarly, the UV-vis spectra of complex **2** also changed after the addition of HS^-, $H_2PO_4^-$, AcO^-, F^- which indicated complex **2** interacted with the above anions (Fig. 3). The spectral responses induced by Cys and GSH were very weak. Interestingly, the interaction of complex **2** with NaHS didn't cause the visible color changes and red-shift phenomenon in spectra changes. The UV-vis spectral changes of complex **4** were similar to that of complex **2** (**S9**).

In order to research the real-life application of synthesized complexes, we also carried out the UV-vis spectral changes in the mixed solvents containing water. Experimental results suggested similar spectral changes of synthesized complexes were also monitored in DMSO-H_2O (9:1, v/v) solution (**S10, S11, S12, S13**), compared with pure DMSO solution. It was found that HS^- also could lead to the color changes of complex (**1**, **3**) in DMSO-H_2O (9:1, v/v) from yellow to red, while other tetrabutylammonium salts could not induce the obvious color changes of the complex solution (Fig. 4). Thus, two complexes (**1**, **3**) can detect HS^- selectively by the naked-eye in aqueous solution which may be applicated in real-life samples.

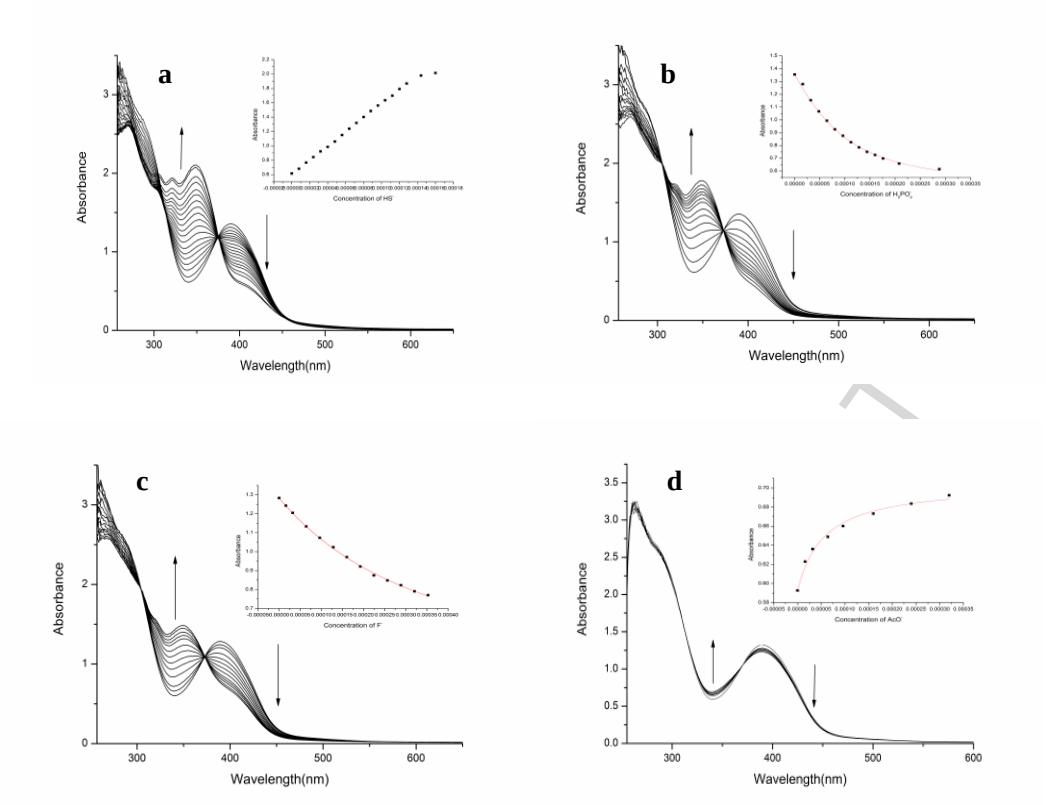

Fig. 3 UV-vis spectral changes of complex **2** upon the addition of various anions. [complex] = 8.0×10^{-5} mol·L^{-1} in DMSO: (a)HS^{-}, (b)$H_2PO_4^{-}$, (c)F^{-}, (d)AcO^{-}. Arrows indicate the direction of increasing anions concentration.

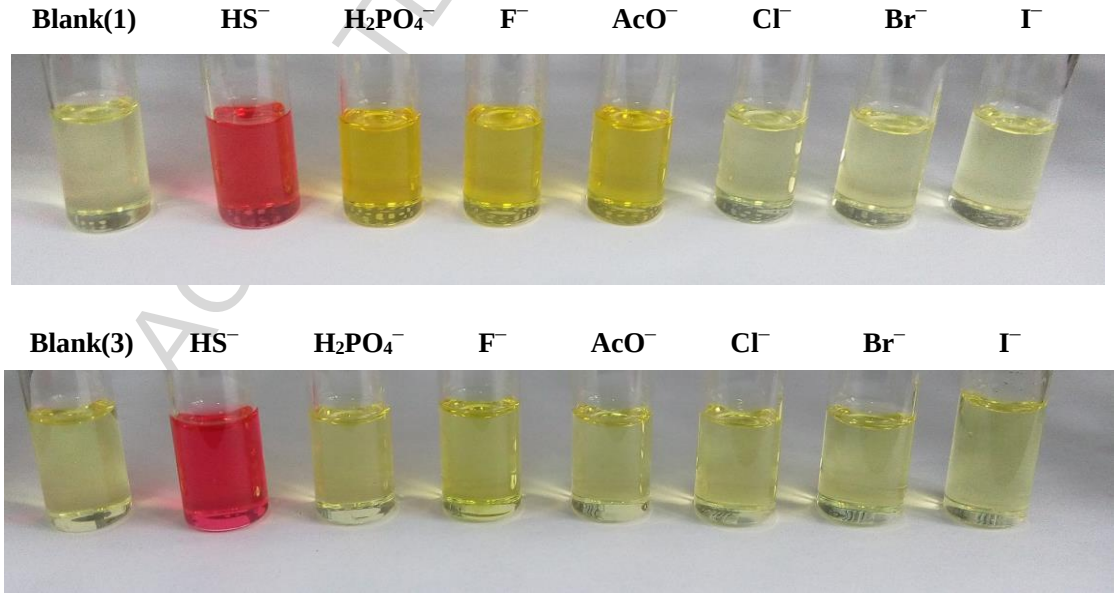

Fig. 4 Photographic images of two complexes (8.0×10^{-5} mol·L^{-1}) and the additions of different anions (8.0 equiv. of complex) in DMSO-H_2O (9:1, v/v).

Furthermore, the detection limit of complex **4** in pure DMSO solution for HS^- was also investigated through UV-vis titration (**S14**). The complex **4** (2.0×10^{-5} mol·L^{-1}) and the concentration of HS^- (0-2.5×10^{-4} mol·L^{-1}) showed a good linear relationship by UV-vis intensity which indicated the quantitative detection of HS^-. The addition of HS^- (1.3×10^{-4} mol·L^{-1}) to the complex **4**, the corresponding UV-vis intensity increased 1.3 times. The above results exhibited the detection limit for HS^- was 1.3×10^{-4} mol·L^{-1}. Also, the time-dependent experiment was conducted (S15). The results indicated that the equilibrium between complex **4** and HS^- completed in two minutes which showed HS^- could be detected quickly.

3.3 Fluorescent response

The fluorescence properties of the Cu(Ⅱ) complex **(4)** were investigated in DMSO-H_2O (9:1, v/v). The free probe displayed weak fluorescence intensity upon excitation at 337 nm. As shown in Fig. 5, with the increasing concentration of HS^-, the fluorescence emission intensity was gradually strengthened at about 430 nm because the added HS^- could coordinate with Cu^{2+} and the free ligand was released. For all quantitative analytical methods, a linear calibration curve is always desired because it allows easy calculation. As shown in Fig. 5(b), a linear relationship ($y=2.495x-118.56$, $R^2=0.9982$, SD=17, N=24) existed between the fluorescence intensity and the concentration (NaHS) in the range of 50-450 μM, indicating that the complex **4** was potentially useful for quantitative analysis of H_2S. The fluorescence titration of complex **4** with various anions was conducted to examine the selectivity. The additions of AcO^-, $H_2PO_4^-$, F^-, Cl^-, Br^-, I^-, SO_4^{2-}, SO_3^{2-}, CO_3^{2-}, Cys and GSH (4.0×10^{-4} mol·L^{-1}) produced a nominal change in the fluorescence spectra of complex

4. All these results suggested that complex **4** was a practical probe for detection of HS^- with high selectivity.

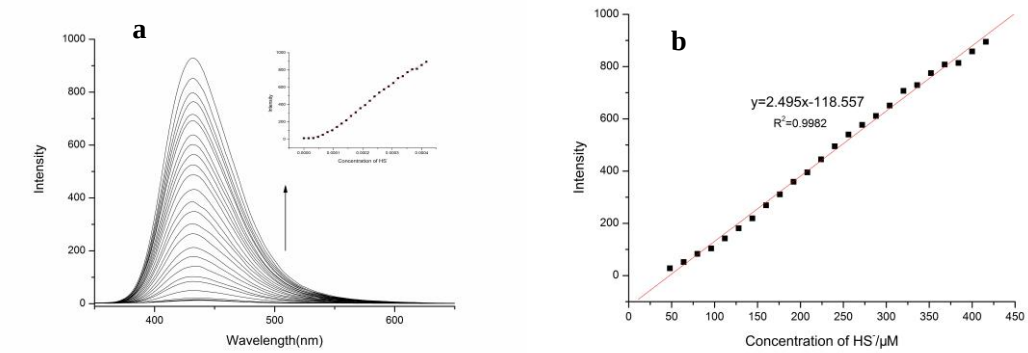

Fig. 5 (**a**) Fluorescence response ($\lambda_{ex,}$ 337nm, slit widths: 5 nm/5 nm) of copper probe **4** (4.0×10^{-5} mol·L^{-1}) upon the addition of NaHS (0 - 4.0×10^{-4} mol·L^{-1}), arrows indicate the increase direction of NaHS concentration. Spectra were acquired in DMSO-H_2O (9:1, v/v) after reaction of the probe with NaHS for 10 min. **(b)** The linearity of increased fluorescence intensity with the concentration of added NaHS in DMSO-H_2O (9:1, v/v).

3.4 Binding constant

Cu(Ⅱ) complexes (**1**, **3**) interacted with HS^- as the ratio of 1:3 and complexes (**2**, **4**) interacted with HS^- as the ratio of 1:1 according to the nonlinear fitting curves. Binding constants of host-guest complexation were calculated according to the equation (1) for 1:3 and equation (2) for 1:1 [54-56].

$$X = X_0 + \Delta\varepsilon c_G c_H^3 \Big/ 1 + K_S c_H^3 \quad (1)$$

$$X = X_0 + \Delta\varepsilon c_G c_H \Big/ 1 + K_s c \quad (2)$$

where, c_G and c_H are the concentrations of guest and host, respectively. X is the

absorbance intensity at certain concentration of host and guest. X_0 is the absorbance intensity of the host alone. K_s is the affinity constant for the host-guest complexation. $\Delta\varepsilon$ is the change in molar extinction coefficient. The binding constants could be obtained and listed in Table 3 based on the UV–vis data. Obviously, the anion binding constants of Cu(Ⅱ) complex in DMSO/H_2O (9:1, v/v) were lower than that in pure DMSO due to the interference of H_2O. The binding constants of AcO^-, with complexes **(3**, **4)** containing naphthylamine cannot be calculated due to the weak spectral changes. However complexes **(1**, **3)** interacted with AcO^- in pure DMSO, it may be related to the steric inhibition of naphthylamine. From Table 3, Cu(Ⅱ) complexes showed the strongest binding ability for HS^- among anions tested. The reason probably was the displacement reaction, in which the Cu^{2+} was captured by HS^- and the free ligand was released from the complex. The above results indicated that the synthesized copper complexes could be used as chemosensors for the detection of HS^- in the sample of environment or pharmacy. Due to the spectral responses were very weak, the binding constants of complexes with Cl^-, Br^-, I^-, SO_4^{2-}, SO_3^{2-}, CO_3^{2-} could not be calculated which suggested the binding abilities were very weak and could be ignored.

3.5 Mechanism

In order to verify the spectral sensing mechanism of copper complexes with NaHS, further insight into the interaction of NaHS with complex was investigated by performing HRMS after the addition of NaHS. As shown in Figure **S16**, after 3 equiv. of NaHS was added, the ion peak of complex **1** ($(M+Na)^+$: 789.7123) was vanished and a new ion peak ($(M-H)^-$: 353.8973) was observed which was the ion peak of free ligand. And so the above results indicated the added HS^- snatched copper cation and the free ligand was released (Scheme 2). Obviously, the similar literatures (H_2S probe

involving metal cation) have been reported [57, 58], the red-shift phenomenon of abs-

Table 3 Binding constants of Cu(Ⅱ) complex with various anions

Anions		K_s (**1**)	K_s (**2**)	K_s (**3**)	K_s (**4**)
HS^-	DMSO	$(2.45\pm0.01)\times10^{4b}$	$(2.36\pm0.08)\times10^{3a}$	$(1.74\pm0.05)\times10^{4b}$	$(2.88\pm0.02)\times10^{3a}$
	aqueous	$(1.28\pm0.01)\times10^{4b}$	$(1.76\pm0.08)\times10^{3a}$	$(1.02\pm0.02)\times10^{4b}$	$(1.91\pm0.06)\times10^{3a}$
$H_2PO_4^-$	DMSO	$(2.71\pm0.09)\times10^{4a}$	$(5.05\pm0.05)\times10^{4a}$	$(5.02\pm0.01)\times10^{4a}$	$(2.14\pm0.01)\times10^{4a}$
	aqueous	$(8.91\pm0.05)\times10^{3a}$	$(2.10\pm0.05)\times10^{4a}$	$(3.93\pm0.30)\times10^{4a}$	$(1.86\pm0.01)\times10^{4a}$
F^-	DMSO	$(1.23\pm0.07)\times10^{4a}$	$(3.27\pm0.08)\times10^{4a}$	$(1.04\pm0.05)\times10^{4a}$	$(1.60\pm0.09)\times10^{4a}$
	aqueous	$(2.98\pm0.07)\times10^{3a}$	$(1.10\pm0.06)\times10^{4a}$	$(6.14\pm0.09)\times10^{3a}$	$(1.03\pm0.01)\times10^{4a}$
AcO^-	DMSO	$(6.37\pm0.01)\times10^{3a}$	$(1.7\pm0.05)\times10^{3a}$	ND[c]	ND
	aqueous	ND	ND	ND	ND
Cys	DMSO	$(4.72\pm0.08)\times10^{3a}$	$(6.36\pm0.05)\times10^{2a}$	$(3.18\pm0.09)\times10^{3a}$	<10
	aqueous	$(2.64\pm0.07)\times10^{3a}$	ND	$(1.07\pm0.94)\times10^{2a}$	<10
GSH	DMSO	ND	<10	ND	<10
	aqueous	ND	ND	ND	<10

[a]The binding ratio of host-guest is 1:1.
[b]The binding ratio of host-guest was 1:3.
[c]The binding constant could not be determined.
Aqueous: the volume of DMSO/H_2O was 9:1.

orbance and the fluorescence enhancement were most likely the reason that the added NaHS could snatch the copper ions from the complex due to the much higher binding constant between sulfide and copper ions. However other anions could only coordinate with complex and form a five-coordinated complex according to comprehensive analysis of UV-vis and fluorescent titration. Why did the complexes (**1**, **3**) interact with HS^- as the ratio of 1:3 and the complexes (**2**, **4**) interact with HS^- as the ratio of 1:1? The binding ratio and binding constants also could illustrate it. As showed in Table 3, the copper complex interacted with HS^- as the ratio of 1:3 in DMSO solution which indicated the copper atom was released from the complex.

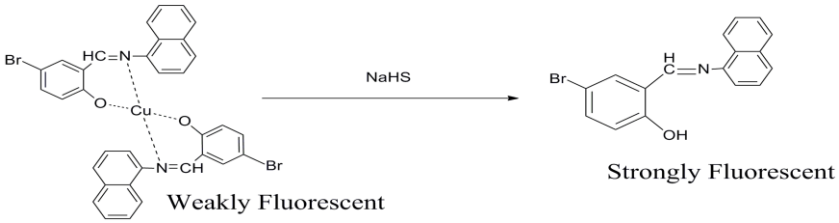

Scheme 2. The possible binding mode for the sensing of HS^-.

3.6 Cytotoxicity test

For further biological application, the quantitative cytotoxicity study of the complex **4** was conducted using the MTT assay. The MTT assay results were collected from Hela cells with complex **4** (2.5 - 80 μg·mL^{-1}). Cell viability was expressed by the ratio between the absorbance of the cells incubated with complex and the cells incubated with blank culture media only. As shown in Fig. 6, the complex **4** showed almost no cytotoxicity to Hela cell at the concentration (80 μg·mL^{-1}) indicating that the complex **4** showed the potential to detect H_2S in cells. Further in vivo studies are currently under way in our laboratory.

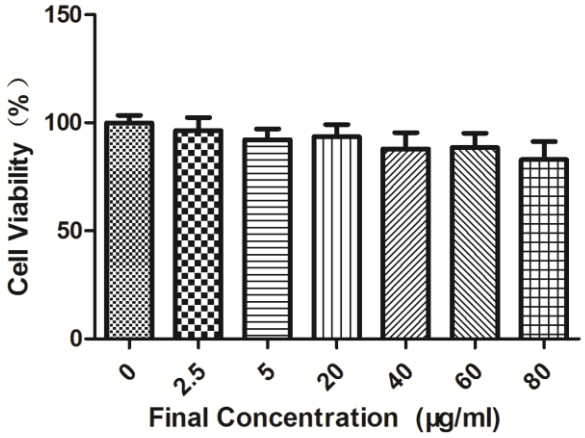

Fig. 6 Cell viability values (%) estimated by MTT proliferation test versus concentrations of complex after 24 h incubation at 37°C. Hela cell was cultured in the 2.5-80 μg·mL^{-1} complex solution at 37°C for 24 h (n=6).

4. Conclusion

In summary, colorimetric fluorescent sensors have been designed and synthesized effectively based on an inorganic-reaction. Two complexes (**1**, **3**) exhibited naked-eye detection for HS^- at room temperature and could be used as colorimetric sensor. Complex **4** displayed a remarkable fluorescence enhancement (over 80-fold) and could be performed as fluorescent OFF–ON probe in DMSO and aqueous solutions. Cytotoxicity studies by Hela cells indicated that complex **4** was low cytotoxicity when the concentration was less than 80 $\mu g \cdot mL^{-1}$. All these features make the synthesized complexes suitable for the direct monitoring of biologically important HS^- in biological samples. The above method was advantage for the simplicity analysis and low cost of the starting material in the present system. The complex holds great potential for environmental analysis of HS^-, S^{2-}, H_2S and their use in bio-analysis is still challenging. Preparation of highly water soluble and highly fluorescent copper complex is under investigation.

Acknowledgment

This work was supported by the Program for Science & Technology Innovation Talents in Universities of Henan Province (15HASTIT039), Fund of Fluorescence Probe and Biomedical Detection Research Team of Xinxiang City (CXTD16001), Scientific and Technological Research Projects of Henan Province (182102311124).

Appendix A. Supplementary data

CCDC 1432286 1432284 1448106 1432281 contains the supplementary crystallographic data for the copper complex **1**, **2**, **3**, **4** reported in this paper. These data can be obtained free of charge via http://www.ccdc.cam.ac.uk/conts/retrieving.html, or from the Cambridge Crystallographic Data Centre, 12 Union Road, Cambridge CB2 1EZ, UK; fax: (+44)

1223-336-033; or e-mail: deposit@ccdc.cam.ac.uk.

Reference

[1] K. Abe, H. Kimura, The possible role of hydrogen sulfide as an endogenous neuromodulator, The Journal of neuroscience, 1996, 16, 1066-1071.

[2] R. Wang, Hydrogen sulfide: the third gasotransmitter in biology and medicine, Antioxidants & redox signaling, 2010, 12, 1061-1064.

[3] M.M. Gadalla, S.H. Snyder, Hydrogen sulfide as a gasotransmitter, Journal of neurochemistry, 2010, 113, 14-26.

[4] R. Wang, Signal Transduction and the Gasotransmitters: NO, CO, and H_2S in Biology and Medicine: Springer Science & Business Media, 2004.

[5] T. Morita, M.A. Perrella, M.-E. Lee, S. Kourembanas, Smooth muscle cell-derived carbon monoxide is a regulator of vascular cGMP, Proceedings of the National Academy of Sciences, 1995, 92, 1475-1479.

[6] L. Li, P. Rose, P.K. Moore, Hydrogen sulfide and cell signaling, Annual review of pharmacology and toxicology, 2011, 51, 169-187.

[7] G. Yang, L. Wu, B. Jiang, W. Yang, J. Qi, K. Cao, et al., H_2S as a physiologic vasorelaxant: hypertension in mice with deletion of cystathionine γ-lyase, Science, 2008, 322, 587-590.

[8] B. Yu, C. Chen, J. Ru, W. Luo, W. Liu, A multifunctional two-photon fluorescent probe for detecting H_2S in wastewater and GSH in vivo. Talanta, 2018, 188, 370-377.

[9] C.K. Nicholson, J.W. Calvert, Hydrogen sulfide and ischemia‐reperfusion injury, Pharmacological Research, 2010, 62, 289-297.

[10] Y.-J. Peng, J. Nanduri, G. Raghuraman, D. Souvannakitti, M.M. Gadalla, G.K. Kumar, et al., H2S mediates O2 sensing in the carotid body, Proceedings of the

National Academy of Sciences, 2010, 107, 10719-10724.

[11] Paul B D, Snyder S H, Role of neuronal signaling effector hydrogen sulfide (H2S) and sulfhydration in Huntington's disease, The FASEB Journal, 2016, 30, 1271-1276.

[12] P. Kamoun, M.C. Belardinelli, A. Chabli, K. Lallouchi, B. Chadefaux - Vekemans, Endogenous hydrogen sulfide overproduction in Down syndrome, American Journal of Medical Genetics Part A, 2003, 116, 310-311.

[13] G. Yang, W. Yang, L. Wu, R. Wang, H_2S, endoplasmic reticulum stress, and apoptosis of insulin-secreting beta cells, Journal of Biological Chemistry, 2007, 282, 16567-16576.

[14] S. Fiorucci, E. Antonelli, A. Mencarelli, S. Orlandi, B. Renga, G. Rizzo, et al., The third gas: H_2S regulates perfusion pressure in both the isolated and perfused normal rat liver and in cirrhosis, Hepatology, 2005, 42, 539-548.

[15] X. Li, C. Yang, K. Wu, Y. Hu, Y. Han, S.H. Liang, A highly specific probe for sensing hydrogen sulfide in live cells based on copper-Initiated fluorogen with aggregation-induced emission characteristics, Theranostics, 2014, 4, 1233-1238.

[16] M.N. Hughes, M.N. Centelles, K.P. Moore, Making and working with hydrogen sulfide: the chemistry and generation of hydrogen sulfide in vitro and its measurement in vivo: a review, Free Radical Biology and Medicine, 2009, 47, 1346-1353.

[17] C. Yu, X. Li, F. Zeng, F. Zheng, S. Wu, Carbon-dot-based ratiometric fluorescent sensor for detecting hydrogen sulfide in aqueous media and inside live cells, Chemical Communications, 2013, 49, 403-405.

[18] Y. Zhao, Y. Yang, L. Cui, F. Zheng, Q. Song, Electroactive Au@Ag nanoparticles driven electrochemical sensor for endogenous H_2S detection, Biosensors & Bioelectronics, 2018, 117, 53-59.

[19] N.S. Lawrence, J. Davis, F. Marken, L. Jiang, T.G. Jones, S.N. Davies, et al., Electrochemical detection of sulphide: a novel dual flow cell, Sensors and Actuators B: Chemical, 2000, 69, 189-192.

[20] J. Zhang, Y. Gao, X. Kang, Z. Zhu, Z. Wang, Z. Xi, L. Yi, o,o-Difluorination of aromatic azide yields a fast-response fluorescent probe for H_2S detection and for improved bioorthogonal reactions. Organic Biomolecular Chemistry, 2017, 15, 4212-4217.

[21] X. Lou, H. Mu, R. Gong, E. Fu, J. Qin, Z. Li, Displacement method to develop highly sensitive and selective dual chemosensor towards sulfide anion, The Analyst, 2011, 136, 684-687.

[22] B.-H. Zhang, F.-Y. Wu, Y.-M. Wu, X.-S. Zhan, Fluorescent method for the determination of sulfide anion with ZnS: Mn quantum dots, Journal of fluorescence, 2010, 20, 243-250.

[23] S.K. Patra, S.K. Sheet, B. Sen, K. Aguan, D.R. Roy, S. Khatua, Highly sensitive bifunctional probe for colorimetric cyanide and fluorometric H_2S detection and bioimaging: Spontaneous resolution, aggregation, and multicolor fluorescence of bisulfide adduct. Journal of Organic Chemistry, 2017, 82, 10234-10246.

[24] H. Tian, J. Qian, H. Bai, Q. Sun, L. Zhang, W. Zhang, Micelle-induced multiple performance improvement of fluorescent probes for H2S detection. Analytical Chimica Acta, 2013, 768, 136-142.

[25] F. Yu, P. Li, P. Song, B. Wang, J. Zhao, K. Han, An ICT-based strategy to a colorimetric and ratiometric fluorescence probe for hydrogen sulfide in living cells, Chemical Communications, 2012, 48, 2852-2854.

[26] X. Shen, C.B. Pattillo, S. Pardue, S.C. Bir, R. Wang, C.G. Kevil, Measurement of plasma hydrogen sulfide in vivo and in vitro, Free Radical Biology and Medicine,

2011, 50, 1021-1031.

[27] C. Gao, X. Liu, X. Jin, J. Wu, Y. Xie, W. Liu, A retrievable and highly selective fluorescent sensor for detecting copper and sulfide, Sensors and Actuators B: Chemical, 2013, 185, 125-131.

[28] Y. Yang, C. Yin, F. Huo, Y. Chu, H. Tong, J. Chao, F. Cheng, A. Zheng. pH-sensitive fluorescent salicylaldehyde derivative for selective imaging of hydrogen sulfide in living cells. Sensors and Actuators B: Chemical, 2013, 186, 212-218.

[29] F.J. Huo, J. Kang, C. Yin, J. Chao, Y. Zhang, Highly selective fluorescent and colorimetric probe for live-cell monitoring of sulphide based on bioorthogonal reaction. Scientific reports, 2015, 5, 8969-.

[30] J. Kang, F. Huo, P. Ning, X. Meng, J. Chao, C. Yin. Two red-emission single and double ‘arms’ fluorescent materials stemed from ‘one-pot’ reaction for hydrogen sulfide vivo imaging. Sensors and Actuators B: Chemical. 2017, 250, 342-350.

[31] F. Huo, Y. Zhang, P. Ning, X. Meng, C. Yin, A novel isophorone-based red-emitting fluorescent probe for selective detection of sulfide anions in water for in vivo imaging. Journal of Materials Chemistry B , 2017, 5, 2798-2803.

[32] Q. Zhao, J. Kang, Y. Wen, F. Huo, Y. Zhang, C. Yin, Turn-on” fluorescent probe for detection of H_2S and its applications in bioimaging. Spectrochimica Acta Part A: Molecular and Biomolecular Spectroscopy, 2018, 189, 8-12.

[33] Q. Zhao, C. Yin, J. Kang, Y. Wen, F. Huo, A viscosity sensitive azide-pyridine BODIPY-based fluorescent dye for imaging of hydrogen sulfide in living cells. Dyes and Pigments, 2018, 159, 166-172.

[34] J. Kang, F. Huo, C. Yin, A novel ratiometric fluorescent H_2S probe based on tandem nucleophilic substitution/cyclization reaction and its bioimaging. Dyes and Pigments, 146, 287-292.

[35] X. Xie, C. Yin, Y. Yue, J. Chao, F. Huo, Fluorescent probe detect distinguishly sulfite/hydrogen sulfide and thiol via two emission channels in vivo. Sensors and Actuators B: Chemical, 2018, 277, 647-653.

[36] Q. Zhao, F. Huo, J. Kang, Y. Zhang, C. Yin, A novel FRET-based fluorescent probe for the selective detection of hydrogen sulfide (H_2S) and its application for bioimaging. Journal of Materials Chemistry B 2018, 6, 4903-4908.

[37] X. Cao, W. Lin, K. Zheng, L. He, A near-infrared fluorescent turn-on probe for fluorescence imaging of hydrogen sulfide in living cells based on thiolysis of dinitrophenyl ether, Chemical Communications, 2012, 48, 10529-10531.

[38] S.J. Li, Y.F. Li, H.W. Liu, D.Y. Zhou, W.L. Jiang, J. Ou-Yang, C.Y. Li, A dual-response fluorescent probe for the detection of viscosity and H_2S and its application in studying their cross-talk influence in mitochondria. Analytical Chemistry, 2018, doi: 10.1021/acs.analchem.8b02068.

[39] J. Li, C. Yin, F. Huo, Chromogenic and fluorogenic chemosensors for hydrogen sulfide: review of detection mechanisms since the year 2009. RSC Advances 2016, 5, 2191-2206.

[40] Y. Yang, C. Yin, F. Huo, Y. Zhang, J. Chao, A ratiometric colorimetric and fluorescent chemosensor for rapid detection hydrogen sulfide and its bioimaging. Sensors and Actuators B: Chemical, 2014, 203, 596-601.

[41] Y. Yang, C. Yin, F. Huo, J. Chao, Y. Zhang, Highly selective relay recognition of hydrogen sulfide and Hg (II) by a commercially available fluorescent chemosensor and its application in bioimaging. Sensors and Actuators B: Chemical, 2014, 204, 402-406.

[42] M.D. Hammers, M.D. Pluth, Ratiometric measurement of hydrogen sulfide and cysteine/homocysteine ratios using a dual-fluorophore fragmentation strategy,

Analytical Chemistry, 2014, 86, 7135-7140.

[43] Y. Chen, C. Zhu, Z. Yang, J. Chen, Y. He, Y. Jiao, et al., A ratiometric fluorescent probe for rapid detection of hydrogen sulfide in mitochondria, Angewandte Chemie, 2013, 125, 1732-1735.

[44] K. Sasakura, K. Hanaoka, N. Shibuya, Y. Mikami, Y. Kimura, T. Komatsu, et al., Development of a highly selective fluorescence probe for hydrogen sulfide, Journal of the American Chemical Society, 2011, 133, 18003-18005.

[45] F. Hou, L. Huang, P. Xi, J. Cheng, X. Zhao, G. Xie, et al., A retrievable and highly selective fluorescent probe for monitoring sulfide and imaging in living cells, Inorganic chemistry, 2012, 51, 2454-2460.

[46] M. Sun, H. Yu, H. Li, H. Xu, D. Huang, S. Wang, Fluorescence Signaling of Hydrogen Sulfide in Broad pH Range Using a Copper Complex Based on BINOL–Benzimidazole Ligands, Inorganic chemistry, 2015, 54, 3766-3772.

[47] A.R. Lippert, E.J. New, C.J. Chang, Reaction-based fluorescent probes for selective imaging of hydrogen sulfide in living cells, Journal of the American Chemical Society, 2011, 133, 10078-10080.

[48] G.-J. Mao, T.-T. Wei, X.-X. Wang, S.-y. Huan, D.-Q. Lu, J. Zhang, et al., High-sensitivity naphthalene-based two-photon fluorescent probe suitable for direct bioimaging of H_2S in living cells, Analytical Chemistry, 2013, 85, 7875-7881.

[49] C. Zou, L. Gao, T. Liu, Z. Xu, J. Cui, A fluorescent probe based on N-butylbenzene-1,2-diamine for Cu(II) and its imaging in living cells, Journal of Inclusion Phenomena & Macrocyclic Chemistry, 2014, 80, 383-390.

[50] X.-F. Shang, H. Lin, Z.-S. Cai, H.-K. Lin, Effects of the receptors bearing phenol group and copper (II) on the anion recognition and their analytical application, Talanta, 2007, 73, 296-303.

[51] R. Hebbachi, N. Benali-Cherif, Bis (trans-(E)-2-{[4-(4-acetylphenylsulfanyl) phenylimino-κN] methyl} phenolato-κO) copper (II), Acta Crystallographica Section E: Structure Reports Online, 2005, 61, 1188-1190.

[52] A. Golcu, M. Tumer, H. Demirelli, R.A. Wheatley, Cd (II) and Cu (II) complexes of polydentate Schiff base ligands: synthesis, characterization, properties and biological activity, Inorganica Chimica Acta, 2005, 358, 1785-1797.

[53] N. Novoa, T. Roisnel, P. Hamon, S. Kahlal, C. Manzur, H.M. Ngo, et al., Four-coordinate nickel (ii) and copper (ii) complex based ONO tridentate Schiff base ligands: synthesis, molecular structure, electrochemical, linear and nonlinear properties, and computational study, Dalton Transactions, 2015, 44, 18019-18037.

[54] Y. Liu, C.-C. You, H.-Y. Zhang, Supramolecular chemistry, Nankai University Publication, Tian Jin, 2001.

[55] J. Bourson, J. Pouget, B. Valeur, Ion-responsive fluorescent compounds. 4. Effect of cation binding on the photophysical properties of a coumarin linked to monoaza- and diaza-crown ethers, Journal of Physical Chemistry, 1993, 97, 457-470.

[56] Y. Liu, C.-C. You, H.-Y. Zhang, Spectroscopic studies on molecular recognition of modified cyclodextrins, Current Organic Chemistry, 2004, 8, 35-46.

[57] S. Palanisamy, L.Y. Lee, Y.L. Wang, Y.J. Chen, C.Y. Chen, Y.M. Wang, A water soluble and fast response fluorescent turn-on copper complex probe for H_2S detection in zebra fish. Talanta, 2016, 147, 445-452.

[58] R. Kaushik, R. Sakla, A. Ghosh, G.T. Selvan, P.M. Selvakumar, D.A. Jose, Selective detection of H_2S by copper complex embedded in vesicles through metal indicator displacement approach. ACS Sensors, 2018, 3, 1142-1148.

Graphical abstract

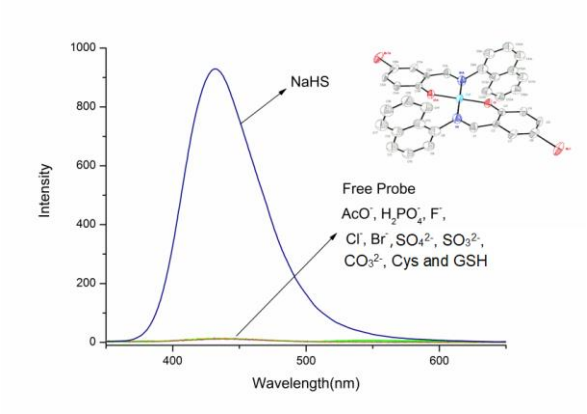

Four crystals based *copper(II)* complexes were obtained and the molecular structures were all characterized by X-ray diffraction. We presented a simple, easily-prepared, yet efficient, inorganic-reaction based sensors for HS^-. An excellent linear relationship and remarkable fluorescence enhancement (over 80-fold) were found in the fluorescent titration of NaHS.

Highlights:

Four crystals based on *copper(II)* complexes were obtained and characterized.

The colorimetric and fluorescence “OFF-ON” probes.

The fluorescent probes were low cytotoxicity Hela cell.

A rapid and convenient detection method for HS^-.